



An approach to preparing porous and hollow metal phosphides with higher hydrodesulfurization activity

Limin Song^a, Shujuan Zhang^{b,*}, Qingwu Wei^a

^a College of Environment and Chemical Engineering & State Key Laboratory of Hollow-fiber Membrane Materials and Membrane Processes, Tianjin Polytechnic University, Tianjin 300160, PR China

^b College of Science, Tianjin University of Science & Technology, Tianjin 300457, PR China

ARTICLE INFO

Article history:

Received 15 December 2010

Received in revised form

13 March 2011

Accepted 29 March 2011

Available online 19 April 2011

Keywords:

Metal

Phosphorus

Metal phosphides

Porous and hollow

Hydrodesulfurization

ABSTRACT

This paper describes an effective method for the synthesis of metal phosphides. Bulk and supported Ni₂P, Cu₃P, and CoP were prepared by thermal treatment of metal and the amorphous red phosphorus mixtures. Porous and hollow Ni₂P particles were also synthesized successfully using this method. The structural properties of these products are investigated using X-ray powder diffraction (XRD), transmission electron microscopy (TEM), scanning electron microscopy (SEM), inductively coupled plasma (ICP–AES) and X-ray photoemission spectroscopy (XPS). A rational mechanism was proposed for the selective formation of Ni₂P particles. In experimental conditions, the Ni₂P/SiO₂ catalyst exhibits excellent hydrodesulfurization (HDS) activity for dibenzothiophene (DBT).

© 2011 Elsevier Inc. All rights reserved.

1. Introduction

Transition metal phosphides have attracted considerable interest for some time because these technologically important materials are used in semiconductors, luminescent devices, electronic components, and hydroprocessing catalysts [1,2]. Transition metal phosphides are attractive candidates especially as HDS catalysts [3–8]. Thus, it is important to develop general synthetic approaches that yield transition metal phosphides. A variety of methods have emerged for the synthesis of these materials including temperature-programmed reduction (TPR) of metal phosphates, treating Ni metal particles with PH₃, solvothermal reactions, as well as high temperature annealing of organometallic and solid-state precursors, etc. [9–23]. In this aspect, it has been reported that the Ni₂P particles were prepared by treating an amorphous Ni–B alloy with phosphine [24]. The as-prepared catalysts exhibited excellent catalytic activity in the HDS of dibenzothiophene. This paper reports a new synthetic route via heat treatment of the mixtures metal and red phosphorus in flowing N₂ to prepare the corresponding metal phosphides (including bulk and supported Ni₂P, Cu₃P, and CoP). At the same time, the HDS of dibenzothiophene was carried out in a flowing fixed-bed reactor for the Ni₂P/SiO₂ catalyst. Although only Ni₂P, Cu₃P, and CoP were synthesized in this study, synthesizing other

bulk and supported metal phosphides is easy via the proposed method. Therefore, the proposed method is a general method for the synthesis of bulk and supported metal phosphides. In comparison with the TPR method, it is simple (facile heat treatment of pure metal and red phosphorus) and short (reaction time is only 0.5 h), making it advantageous to the synthesis of metal phosphide catalysts. In addition, porous and hollow Ni₂P particles may be obtained successfully using the proposed method, indicating the possibility to synthesize metal phosphides with special morphologies.

2. Experimental

Commercially available solvents and reagents were used without further purification. All the reagents were purchased from Tianjin Guangfu Fine Chemical Research Institute (Tianjin, China). The purity of metal and red phosphorus powder is 99.9% (AR). Tube furnace is a home-made device with 2000 W of heating power (Fig. 1). In a typical preparation process, the precursors were prepared by mixing metal (Ni, Cu, and Co) and red phosphorus (P) powder with the molar ratio of metal to phosphorus being 1/2. The above precursors were heated to 700 °C at a rate of 20 °C/min in a flowing N₂ with a rate of 10 mL/min. The reaction was maintained for 0.5 h at 700 °C, and then the products were cooled to room temperature. Finally, the samples were passivated in a flow of 1 vol% O₂/N₂. The yields of the Ni₂P, Cu₃P, and CoP samples are about 63%, 56%, and 51% when the

* Corresponding author. Fax: +86 22 60600658.

E-mail address: zhangshujuan@tust.edu.cn (S. Zhang).

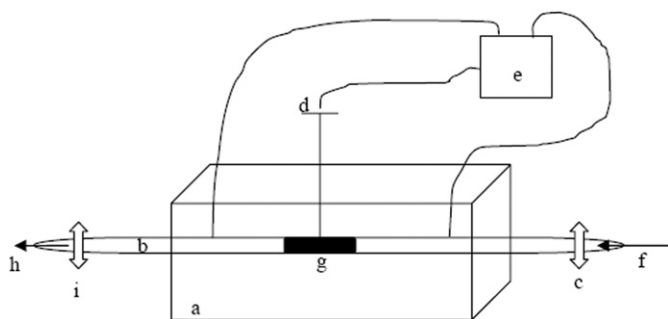


Fig. 1. Apparatus of tube furnace. (a) furnace body; (b) quartz tube; (c) valve; (d) thermocouple; (e) controller; (f) N₂ intake; (g) quartz boat, (h) N₂ uptake; and (i) valve.

molar ratio of metal to phosphorus is 1/2, respectively. In the experiment, a part of the excess phosphorus was transported out of the reaction by N₂ flow. Another part of phosphorus in the form of white phosphorus deposited at the cool end of the tube. In the reaction, the allotrope phosphorus is highly toxic and flammable. These experiments require careful operation with precautions. The paper wiping the nozzle should be put into cold water to prevent fire.

The precursors of Ni₂P/SiO₂ catalysts (with metal loadings equivalent to 10.2 wt%) were prepared as follows. Prior to use, the silica support was calcined in air at 773 K for 3 h. The silica was then impregnated with an aqueous solution of Ni powder under stirring, and followed by drying for 3 h at 393 K. The above SiO₂ and red phosphorus with the molar ratio of metal to phosphorus being 1/2 were mechanically mixed to obtain the precursor. Other steps are similar to prepare bulk Ni₂P.

The products were characterized using X-ray diffraction (XRD) recorded on a Rigaku D/max 2500 powder diffractometer equipped with monochromatic high-intensity CuK α radiation ($\lambda=1.5406$ Å). The morphology and size of the as-prepared products were observed by a Hitachi H-7650 transmission electron microscopy (TEM) and a Hitachi S-4800 scanning electron microscope (SEM). The elemental content of the samples was determined using the inductively coupled plasma (ICP–AES, 9000(N+M)) method. The binding energy (BE) was measured by an X-ray photoelectron spectrometer (XPS, Pekin-Elmer PHI5300). In the XPS analysis, the calibration of BE is the standard peak of adventitious carbon (C_{1s}). The BE has been calibrated according to the standard peak of carbon (C_{1s}) in the manuscript.

The HDS of dibenzothiophene was carried out in a flowing fixed-bed reactor using a feed consisting of a decalin solution of DBT (0.5 wt%). The conditions of the HDS reaction were 330 °C, 3.0 MPa, WHSV=9 h⁻¹, and H₂ flow rate 90 ml min⁻¹. 1.0 mL (0.6 g) of Ni₂P/SiO₂ catalyst diluted with quartz sands to 5.0 mL was reduced by heating from room temperature to a certain temperature in H₂ (200 mL min⁻¹), maintaining the sample at that temperature for 2 h, before changing the temperature to the desired reaction temperature. Liquid samples were collected every hour and analyzed by a gas chromatography with a flame ionization detector (FID) and a capillary column (OV101). The DBT conversion was used as a measure of the HDS activity [15].

3. Results and discussion

Fig. 2 shows the X-ray diffraction (XRD) patterns of as-prepared bulk products. All diffraction peaks of the three samples are attributed to the corresponding Ni₂P ($2\theta=17.52^\circ, 26.36^\circ, 30.56^\circ, 31.82^\circ, 35.40^\circ, 40.74^\circ, 44.64^\circ, 47.40^\circ, 54.18^\circ, 55.00^\circ, 63.46^\circ, 66.36^\circ, 69.92^\circ, 72.70^\circ, 74.72^\circ$), Cu₃P ($2\theta=28.64^\circ, 29.16^\circ,$

$36.16^\circ, 39.24^\circ, 41.76^\circ, 45.28^\circ, 46.32^\circ, 47.46^\circ, 52.38^\circ, 53.64^\circ, 56.68^\circ, 59.20^\circ, 66.72^\circ, 69.38^\circ, 73.58^\circ,$ and 78.50°), and CoP ($2\theta=23.66^\circ, 31.64^\circ, 32.00^\circ, 35.38^\circ, 36.36^\circ, 36.68^\circ, 38.96^\circ, 45.18^\circ, 46.26^\circ, 48.16^\circ, 52.26^\circ, 56.06^\circ, 56.80^\circ, 61.72^\circ, 64.20^\circ, 66.02^\circ, 68.02^\circ, 68.86^\circ, 74.78^\circ, 75.90^\circ, 76.34^\circ,$ and 77.16°) with hexagonal, hexagonal, and orthorhombic structures, respectively (JCPDS Card No. 89-4864, 71-2261, and 89-4862). No other reflections (including oxides and other phosphide phases) were found in the XRD patterns indicating pure Ni₂P, Cu₃P, and CoP products.

To study the effect of Ni/P ratios on the product, the formation of Ni₂P is investigated. **Fig. 3** presents the XRD patterns of the resultant Ni₂P samples from precursors with different Ni/P ratios. At Ni/P molar ratio 2/1 (**Fig. 3a**), all diffraction peaks corresponding to the hexagonal Ni₂P ($2\theta=17.50^\circ, 26.34^\circ, 30.52^\circ, 31.78^\circ, 35.38^\circ, 40.72^\circ, 44.60^\circ, 47.36^\circ, 54.16^\circ, 54.96^\circ, 63.42^\circ, 66.34^\circ, 69.88^\circ, 72.66^\circ,$ and 74.70°) are observed, which is identified as pure Ni₂P. At Ni/P molar ratio 1/1 and 1/2 (**Fig. 3b** and **c**), the diffraction peaks of Ni₂P are very strong and no other peaks appear. This indicates that Ni is transformed into Ni₂P completely at this Ni/P ratio. With a further decrease on Ni/P molar ratio

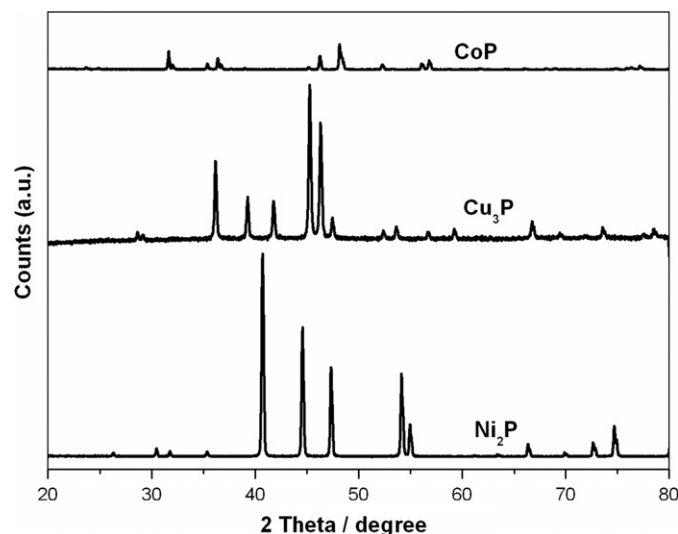


Fig. 2. X-ray diffraction patterns of bulk Ni₂P, Cu₃P, and CoP treated at 700 °C for 0.5 h. The molar ratio of metal to phosphorus is 1/2.

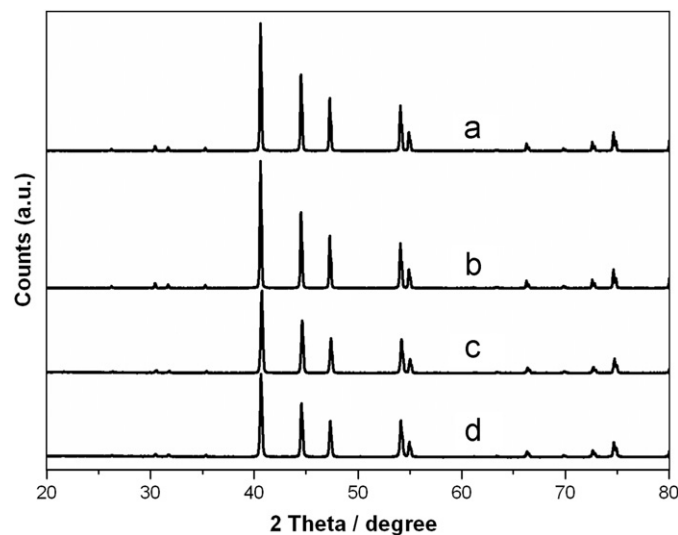


Fig. 3. X-ray diffraction patterns of bulk Ni₂P with different Ni/P ratios treated at 700 °C for 0.5 h. (a) 2:1, (b) 1:1, (c) 1:2, and (d) 1:3.

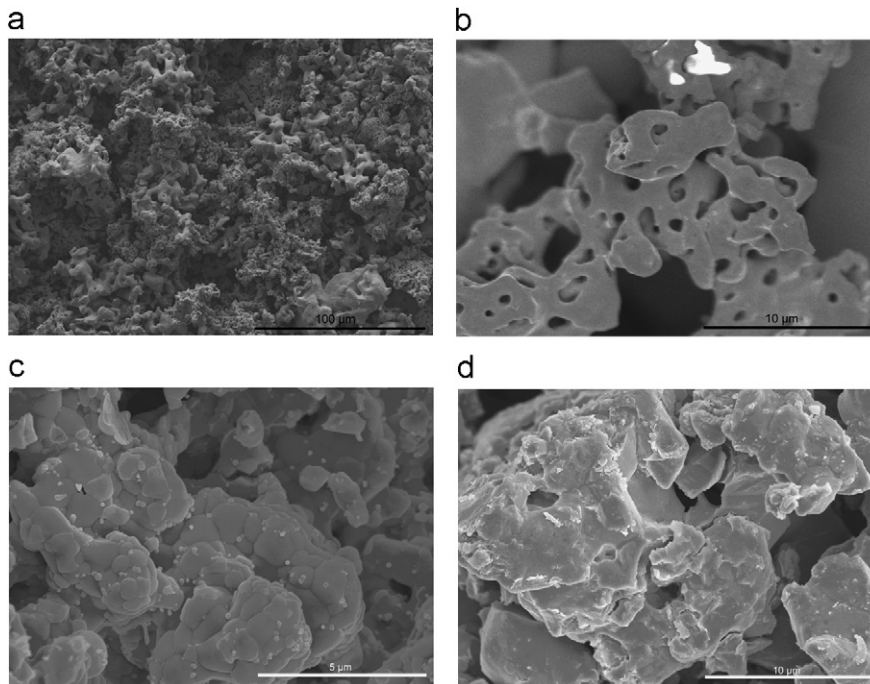


Fig. 4. FESEM images of bulk Ni_2P , CoP, and Cu_3P treated at 700°C for 0.5 h. The molar ratio of metal to phosphorus is 1/2. (a and b) Ni_2P , (c) CoP, and (d) Cu_3P .

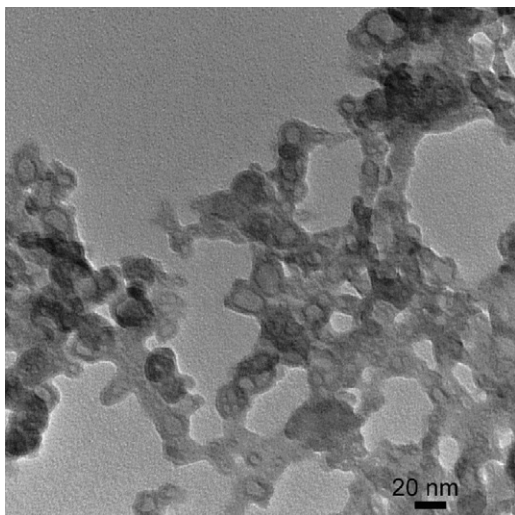


Fig. 5. TEM images of bulk Ni_2P treated at 700°C for 0.5 h. The molar ratio of metal to phosphorus is 1/2.

($\text{Ni}/\text{P}=1/3$) (Fig. 3d), pure Ni_2P phase is still produced. This result indicates that Ni powder reacts with red phosphorus powder easily under experimental conditions to form a well-crystallized Ni_2P phase if the Ni/P ratio is smaller than 2/1. The melting point of red phosphorus is 590°C . The solid red phosphorus was transformed into gaseous phosphorus when the reaction was carried out at 700°C . Therefore, superfluous phosphorus evaporates and drains along with the N_2 current after reacting with Ni and red phosphorus powder. The pure Ni_2P phase can be obtained successfully as long as the Ni/P ratio is smaller than 2/1.

Fig. 4 presents the field emission scanning electron microscopy images of the bulk Ni_2P , CoP, and Cu_3P . It is clear that the particles of Ni_2P are not uniform and composed of many small granules (Fig. 4a). The particle sizes vary in the range 1–5 μm . Interestingly, the interior of particles is hollow and the surface has many pores (Fig. 4b). From Fig. 4c, we can see the CoP particles are

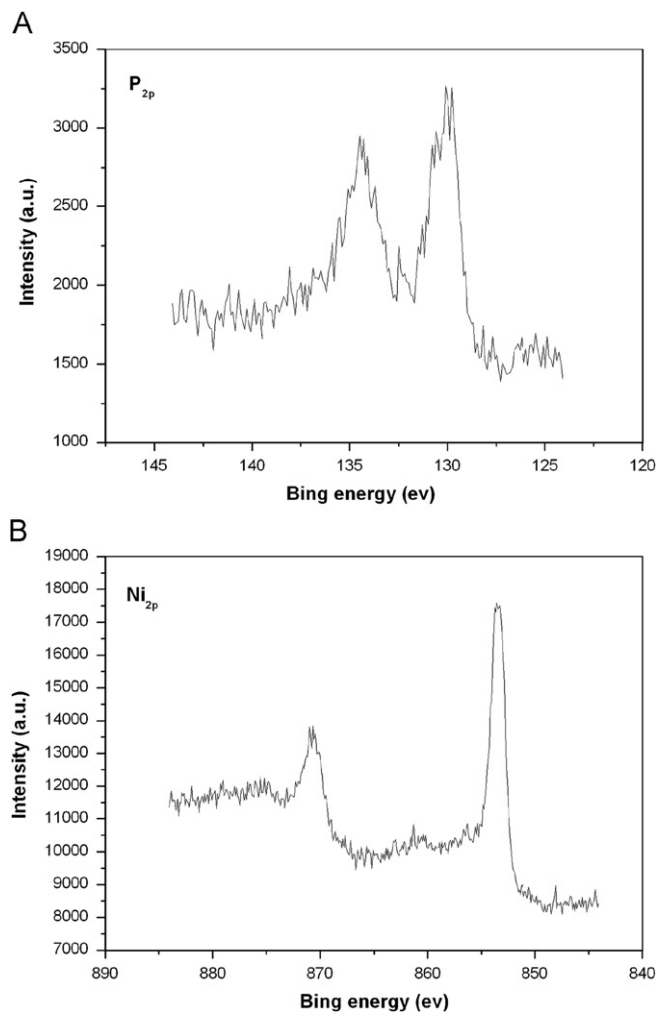


Fig. 6. X-ray photoelectron spectra (XPS) for the Ni_2P precursor treated at 700°C for 0.5 h in a flowing N_2 (the molar ratio of metal to phosphorus is 1/2). (A), P_{2p} (B) Ni_{2p} .

accumulated by small particles with the size of 0.5–1 μm . However, there are no obvious pores in the surface. From Fig. 4d, the Cu_3P particles are the large particles of solid with micron size. To investigate the size of the Ni_2P granules and its internal structure, transmission electron microscopy images were obtained (Fig. 5). From Fig. 5, the actual size of granules is about 20 nm, the interior is truly hollow and the surface is porous.

In nanoparticle reactions there is a popular mechanism for hollow particle formation as inner material from a solid particle migrates to the exterior. For the formation mechanism of the hollow Ni_2P particles, we speculated that it might be the first reaction of red phosphorus and nickel on the surface of metal particles to form Ni_2P . The red phosphorus at this time is liquid or gaseous because the reaction temperature is higher than the melting point of red phosphorus, therefore, the resultant Ni_2P is a loose structure. The liquid or gaseous red phosphorus goes into the interior of loose Ni_2P particles, and continue to react with nickel cores to form Ni_2P , which ultimately leads to the formation of hollow structure.

Fig. 6 shows the P_{2p} (Fig. 6A) and Ni_{2p} (Fig. 6B) XPS spectra of the as-synthesized Ni_2P sample. The peak at 130.0 eV is attributed to P atoms in Ni_2P [25], while the peaks at higher BE values (134.4 eV) are attributed to oxides which are more pronounced in the as-received sample [26]. The single and narrow peak at 853.4 eV is assigned to the Ni cations in Ni_2P [25]. The broad

peak centered at 871.0 eV on the high binding-energy side is assigned to the Ni_{2p} signal from oxidized Ni species [27]. Quantitative analysis was performed using the intensities of the P_{2p} and Ni_{2p} spectra normalized by their atomic sensitivity factors. It was found that Ni/P is 0.73. The apparent P excess is an indication of the existence of oxidized P in the Ni_2P particles.

To investigate the hydrotreating activity of the Ni_2P synthesized by the proposed route, the SiO_2 -supported Ni_2P catalyst ($\text{Ni}_2\text{P}/\text{SiO}_2$) was prepared and tested by the HDS of dibenzothio-*phene*. The Ni loading in the $\text{Ni}_2\text{P}/\text{SiO}_2$ samples was 10.2 wt%. The bulk and supported compositions of as-prepared samples are determined by inductively coupled plasma analysis. The average mole ratio of Ni to P in the as-prepared bulk and supported Ni_2P samples is 1.86 and 1.93, respectively. Fig. 7 shows the XRD patterns of the bulk Ni_2P , SiO_2 support, and $\text{Ni}_2\text{P}/\text{SiO}_2$. The XRD pattern of the support shows that the SiO_2 powder is amorphous because of the lack of sharp peaks. The sharp peaks of $\text{Ni}_2\text{P}/\text{SiO}_2$ are attributed to the Ni_2P phase ($2\theta=30.32^\circ$, 31.56° , 31.70° , 40.56° , 44.46° , 47.22° , 52.84° , 54.02° , 54.84° , 66.22° , 69.82° , 72.54° , and 74.60°). Fig. 8 gives the TEM images of the SiO_2 supported Ni_2P samples. From Fig. 8a, it is very clear that most of the as-synthesized Ni_2P particles have a hollow structure and the size is about 10–30 nm. The size of the Ni_2P particles obtained by TPR method is around 30–50 nm in Fig. 8b. Comparing the two

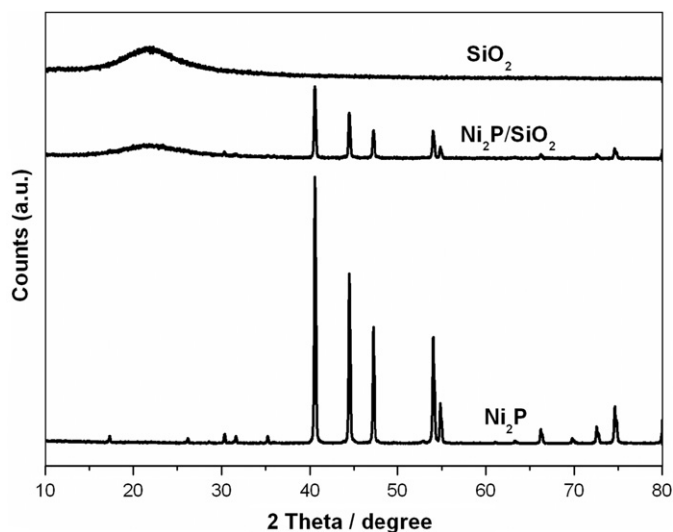


Fig. 7. X-ray diffraction patterns of bulk and SiO_2 supported Ni_2P treated at 700°C for 0.5 h. The molar ratio of metal to phosphorus is 1/2.

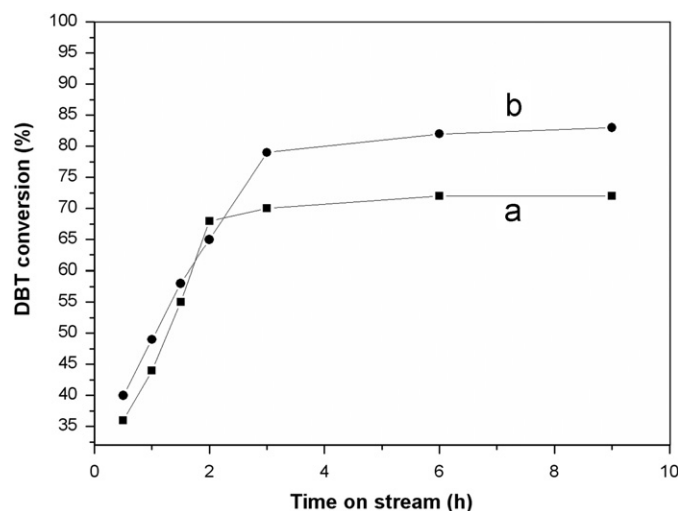


Fig. 9. Effect of reaction time on the HDS activity of the $\text{Ni}_2\text{P}/\text{SiO}_2$ at 320°C . (a) The TPR method and (b) the new method. Ni loadings = 10.2 wt%.

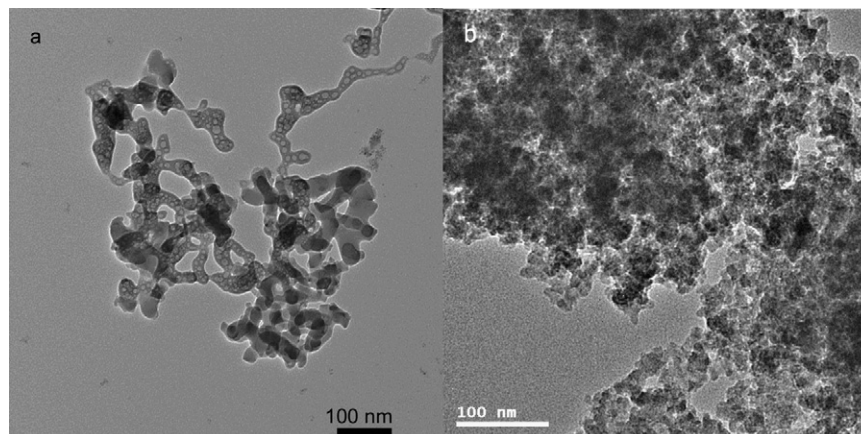


Fig. 8. TEM images of $\text{Ni}_2\text{P}/\text{SiO}_2$ treated at 700°C for 0.5 h. (a) Ni and red phosphorus powder (the molar ratio of metal to phosphorus is 1/2) and (b) the TPR method.

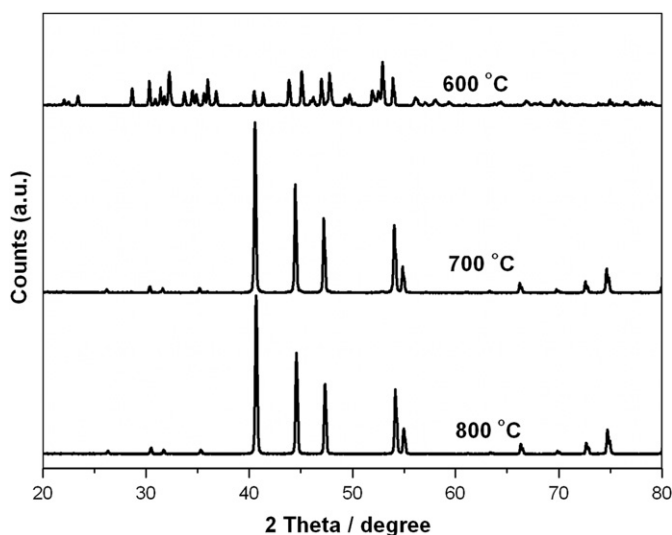


Fig. 10. X-ray diffraction patterns of bulk Ni₂P treated at different temperature for 0.5 h. The molar ratio of metal to phosphorus is 1/2.

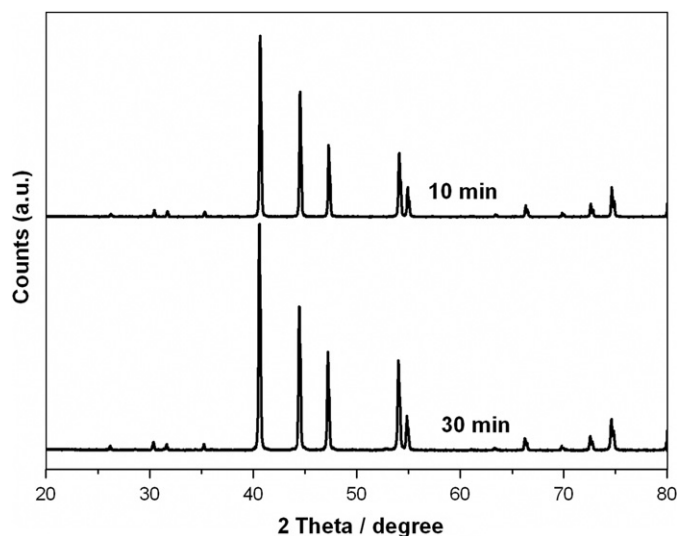


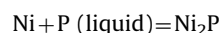
Fig. 11. X-ray diffraction patterns of bulk Ni₂P treated at 700 °C for different time. The molar ratio of metal to phosphorus is 1/2.

catalysts, the as-synthesized Ni₂P/SiO₂ can provide a higher surface area and more active sites, which will help to improve the desulfurization activity. The data of Ni₂P/SiO₂ catalysts for the HDS of dibenzothiophene are listed in Fig. 9. HDS activity reached 83% in the experimental condition; this is much higher than that of Ni₂P/SiO₂ prepared by the TPR method (72%).

To study the reaction mechanism, the reactions with Ni and red phosphorus powder were carried out at different temperatures and time. Fig. 10 shows the XRD peaks of the Ni₂P samples with different preparation temperatures. The obtained product is pure phase Ni₂P ($2\theta=17.46^\circ, 26.30^\circ, 30.48^\circ, 31.74^\circ, 35.34^\circ, 40.68^\circ, 44.58^\circ, 47.34^\circ, 54.14^\circ, 54.94^\circ, 61.16^\circ, 63.38^\circ, 66.32^\circ, 69.86^\circ, 72.66^\circ, \text{ and } 74.70^\circ$) without other impurity when the reaction temperature is 700 °C or 800 °C. When the temperature decreases to 600 °C, the peaks of many species including Ni₂P, Ni₃P, Ni₅P₄, and Ni₈P₃ appear. Fig. 11 gives the XRD peaks of the Ni₂P samples treated at 700 °C for 10 and 30 min. Compared with

the two samples XRD peaks, all the XRD peaks can be in agreement with the Ni₂P standard patterns (JCPDS Card No. 89-4864). This indicates that we are still able to obtain pure Ni₂P when the reaction time reduced to 10 min.

The solid–liquid–gas phases of red phosphorus may coexist under the reaction condition because the melting point of red phosphorus is 590 °C. Since Ni₂P was obtained at Ni/P at 2/1 (Fig. 3a) and there is a N₂ flow to remove the vapor, and pure phosphorus was still expected to leave in the product when extra phosphorus was used as reactant (Fig. 6), it is more likely that the evaporation of phosphorus is not very significant. So solid–liquid–gas should coexist under the reaction condition. Since gas will be carried away by the N₂ flow, the reaction is possible happens on solid metal and liquid phosphorus interface. The liquid phosphorus reacts with Ni according to the following pathway:



The reaction does not carry out completely and forms many other outgrowths because the reaction temperature of 600 °C just surpasses the melting point of red phosphorus.

4. Conclusions

In summary, bulk and supported Ni₂P, Cu₃P, and CoP can be prepared by heat treating of metal and red phosphorus powder. The method is simple, timesaving, and universal to synthesize corresponding metal phosphide catalysts. The as-prepared Ni₂P/SiO₂ catalyst exhibits good HDS activity for dibenzothiophene HDS. In addition, the hollow and porous particles of Ni₂P can be prepared by the proposed route, resulting to a much larger surface area and more active sites in which the Ni₂P catalyst can show better activity for dibenzothiophene HDS.

References

- [1] D.C. Phillips, S.J. Sawhill, R. Self, M.E. Bussell, *J. Catal.* 207 (2002) 266.
- [2] W.R.A.M. Robinson, J.N.M. van Gestel, T.I. Koranyi, S. Eijssbouts, A.M. van der Kraan, J.A.R. van Veen, V.H.J. de Beer, *J. Catal.* 161 (1996) 539.
- [3] S.T. Oyama, *J. Catal.* 216 (2003) 343.
- [4] P.A. Clark, S.T. Oyama, *J. Catal.* 218 (2003) 78.
- [5] S.T. Oyama, Y.-K. Lee, *J. Catal.* 258 (2008) 393.
- [6] A. Wang, M. Qin, J. Guan, L. Wang, H. Guo, X. Li, Y. Wang, R. Prins, Y. Hu, *Angew. Chem. Int. Ed.* 47 (2008) 6052.
- [7] Y.-K. Lee, S.T. Oyama, *J. Catal.* 239 (2006) 376.
- [8] S.T. Oyama, X. Wang, Y.K. Lee, et al., *J. Catal.* 221 (2004) 263.
- [9] V.B. Chernogorenko, S.V. Muchnik, K.A. Lynchak, Z.A. Klimak, V.G. Ivanchenko, *Mater. Res. Bull.* 16 (1981) 1.
- [10] J.W. Liu, X.Y. Chen, M.W. Shao, C.H. An, W.C. Yu, Y.T. Qian, *J. Cryst. Growth* 252 (2003) 297.
- [11] Q.X. Guan, W. Li, M.H. Zhang, K.Y. Tao, *J. Catal.* 263 (2009) 1.
- [12] S. Yang, C. Liang, R. Prins, *J. Catal.* 237 (2006) 118.
- [13] H. Loboué, C. Guillot-Deudon, A. Florin Popa, A. Lafond, B. Rebours, C. Pichon, T. Cseri, G. Berhault, C. Geantet, *Catal. Today* 130 (2008) 63.
- [14] A.E. Henkes, Y. Vasquez, R.E. Schaak, *J. Am. Chem. Soc.* 129 (2007) 1896.
- [15] Z.Q. Wang, L.X. Zhou, M.H. Zhang, M. Su, W. Li, K.Y. Tao, *Chem. Asian J.* 4 (2009) 1794.
- [16] G.J. Shi, J.Y. Shen, *J. Mater. Chem.* 19 (2009) 2295.
- [17] L.N. Ding, M.Y. Zheng, A.Q. Wang, T. Zhang, *Catal. Lett.* 135 (2010) 305.
- [18] Y.H. Ni, A.L. Tao, G.Z. Hu, X.F. Cao, X.W. Wei, Z.S. Yang, *Nanotechnology* 17 (2006) 5013.
- [19] Y.H. Ni, K.M. Liao, J. Li, *Cryst. Eng. Commun.* 12 (2010) 1568.
- [20] Y.H. Ni, J. Li, L.N. Jin, J. Xia, J.M. Hong, K.M. Liao, *New J. Chem.* 33 (2009) 2055.
- [21] J. Li, Y.H. Ni, K.M. Liao, J.M. Hong, *J. Colloid Interf. Sci.* 332 (2009) 231.
- [22] Y.H. Ni, J. Li, L. Zhang, *Mater. Res. Bull.* 44 (2009) 1166.
- [23] Y.H. Ni, L.N. Jin, J.M. Hong, *Nanoscale* 3 (2011) 196.
- [24] L.M. Song, W. Li, G.L. Wang, M.H. Zhang, K.Y. Tao, *Catal. Today* 125 (2007) 137.
- [25] X.P. Duan, Y. Teng, A.J. Wang, V.M. Kogan, X. Li, Y. Wang, *J. Catal.* 261 (2009) 232.
- [26] T. Korányi, *Appl. Catal. A Gen.* 239 (2003) 253.
- [27] E.E. Khawaja, M.A. Salim, M.A. Khan, F.F. Al-Adel, G.D. Khattak, Z. Hussain, *J. Non-cryst. Solids* 110 (1989) 33.